JMEPEG (2014) 23:1576–1579
DOI: 10.1007/s11665-014-0921-z

1059-9495/$19.00

Self-Diffusion in Grain Boundaries and Dislocation Pipes in Al, Fe, and Ni and Application to AlN Precipitation in Steel

G. Stechauner and E. Kozeschnik

(Submitted October 15, 2013; in revised form January 7, 2014; published online February 27, 2014)

Diffusion along microstructural defects, such as grain boundaries or dislocation pipes, is significantly faster than diffusion through an undisturbed crystal. The ratio of diffusion enhancement is 3-4 orders of magnitude close to the melting point and reaches up to several ten orders of magnitude close to room temperature. An assessment of literature shows a large scatter in the available data and emphasizes the need for representative mean values. Applying a least mean square fit to selected experimental information delivers temperature-dependent functions for the ratio of grain boundary and dislocation pipe to bulk diffusion, respectively. We demonstrate that application of the attained results in a computational framework for the kinetics of precipitation makes the predictive simulation possible for the evolution of particles located at dislocations and grain boundaries.

Keywords carbon/alloy steels, diffusion, dislocation, grain boundary, thermokinetic simulation

1. Introduction

Diffusion in solids is a well-known phenomenon and has been investigated heavily over the last decades. Accurate assessments of bulk self-diffusion in Al and Ni have been performed by Campbell (Ref 1) and in Fe by Fridberg et al. (Ref 2) and Jönsson (Ref 3), respectively. The assessed data for the bulk diffusion rates, that is diffusion in an equilibrated and defect-poor alloy, lie predominantly within a narrow confidence band and are generally in good agreement with each other. However, the acceleration of diffusion kinetics along short-circuit paths, such as grain boundaries or dislocation pipes, is rather complex. Data and publications on this topic are sparse in some systems, and the scatter of data can be in the range of several orders of magnitude. Simple temperature extrapolation of individual sets of data is not advisable and, even within the measured temperature range, uncertainties remain.

This article is an invited submission to JMEP selected from presentations at the Symposia "Wetting," "Interface Design," and "Joining Technologies" belonging to the Topic "Joining and Interface Design" at the European Congress and Exhibition on Advanced Materials and Processes (EUROMAT 2013), held September 8-13, 2013, in in Sevilla, Spain, and has been expanded from the original presentation.

G. Stechauner, Materials Center Leoben Forschung GmbH, Leoben, Austria; and **E. Kozeschnik**, Christian Doppler Laboratory for Early Stages of Precipitation, Institute of Materials Science and Technology, Vienna University of Technology, Vienna, Austria. Contact e-mail: georg.stechauner@tuwien.ac.at.

Kaur and Gust (Ref 4) have reviewed grain boundary and dislocation pipe diffusion data in the eighties. Since then, a handful of newer experiments have become available, which are taken into account in the present assessment. After analysis of the dislocation and grain boundary diffusion coefficients obtained in our analysis, these results are utilized in a study of AlN formation along grain boundaries and dislocations in microalloyed steel.

2. Experimental Challenges

Obtaining reliable values for diffusion coefficients over a wide range of temperatures is a challenging task. Several effects must be taken into account that can lead to unavoidable scatter in the data. Whereas the bulk diffusion rate is a quantity that can be obtained experimentally by relatively easy means, grain boundary and, even more so, dislocation pipe self-diffusion are dependent on various factors and they are significantly more difficult to measure. One major reason in this context is the tremendous effect of material purity on the diffusion rate. Whereas older research (Ref 5) is sometimes contradicting more recent publications (Ref 6-8), it seems accepted, nowadays, that an increase in purity will increase the resulting diffusion rates, for instance, along grain boundaries. In addition to purity, the misorientation of the grain boundary is an important factor, carrying even the possibility of the occurrence of coincidence site lattices. An increase in misorientation generally increases the diffusion rate, as long as no coincidence site lattices occur (Ref 9). Consequently, even experiments that are very similar in purity and other parameters yield a considerable scatter.

The use of radiotracers and serial sectioning is the method of choice in Ni and Fe system, where the isotopes ^{63}Ni and ^{59}Fe are readily available. For the Al system, tracer self-diffusion measurements are difficult to obtain because the only useful

tracer isotope is ^{26}Al. Since this isotope has a half-life of 7.4×10^5 years, the number of radioactive counts available in the experiment is rather low (Ref 9). Complex investigation methods must generally be applied to gather data on Al self-diffusion (Ref 10, 11). Detailed information on this issue is reported in ref. (Ref 4). For the diffusion along fcc-Fe dislocation pipes, no experimental data are accessible to the authors. Consequently, in the present work, we assume that this quantity has a similar value as that for Ni, as they share the same crystal structure and a melting temperature in the same order of magnitude.

3. Statistical Analysis

The original data sources for Ni (Ref 7, 12-15), Al (Ref 10, 11, 16), bcc-Fe (Ref 5, 17-19), and fcc-Fe (Ref 20-22) short-circuit self-diffusion are plotted in Figure 1. For the sake of clarity, we show the experimental diffusion rates only at the reported maximum/minimum temperature as obtained from the Q and D_0 values given in the respective literature sources. Details on the assessment procedure are reported elsewhere (Ref 23).

The fits are performed in such a way that a single mathematical equation describes the data over the entire temperature regime. For bcc-Fe, three separate regions need to be accounted for to consider the transition from ferro- to para-magnetic ordering. The following Tables 1 and 2 summarize the values for activation energy and pre-exponential factor, which are used here to calculate the diffusion ratio $D_{GB}/D_{Bulk} = D_{0,GB}/D_{0,Bulk} \times \exp(-(Q_{GB}-Q_{Bulk})/RT)$. The ratio for D_{Disl}/D_{Bulk} can be obtained likewise by using Q and D_0 for dislocation pipes.

4. Application to AlN Precipitation at Grain Boundaries and Dislocations of Microalloyed Steel

Precipitation of carbides and nitrides in microalloyed steel is of high technical relevance, since the interaction of precipitates and dislocations provides one of the major strengthening mechanisms in metals (Ref 24). In addition, precipitates can pin grain boundaries and, thus, provide a convenient means for controlling grain size evolution during heat treatment.

With the thermokinetic software package MatCalc (http://matcalc.at), which is developed for the simulation of precipitation kinetics in multi-component systems, the evolution of AlN precipitates in microalloyed steel is calculated. We utilize the thermodynamic database mc_fe.tdb (Ref 25) and the mobility database mc_fe.ddb (Ref 26), which are based on the CALPHAD approach, to evaluate the precipitation kinetics of the AlN particles at dislocations and grain boundaries. We have chosen this example because Al impurity diffusion is linked linearly to the self-diffusion coefficient of Fe, as documented in the work of Fridberg et al (Ref 2). The diffusion data and ratios reported in the previous section are implemented for

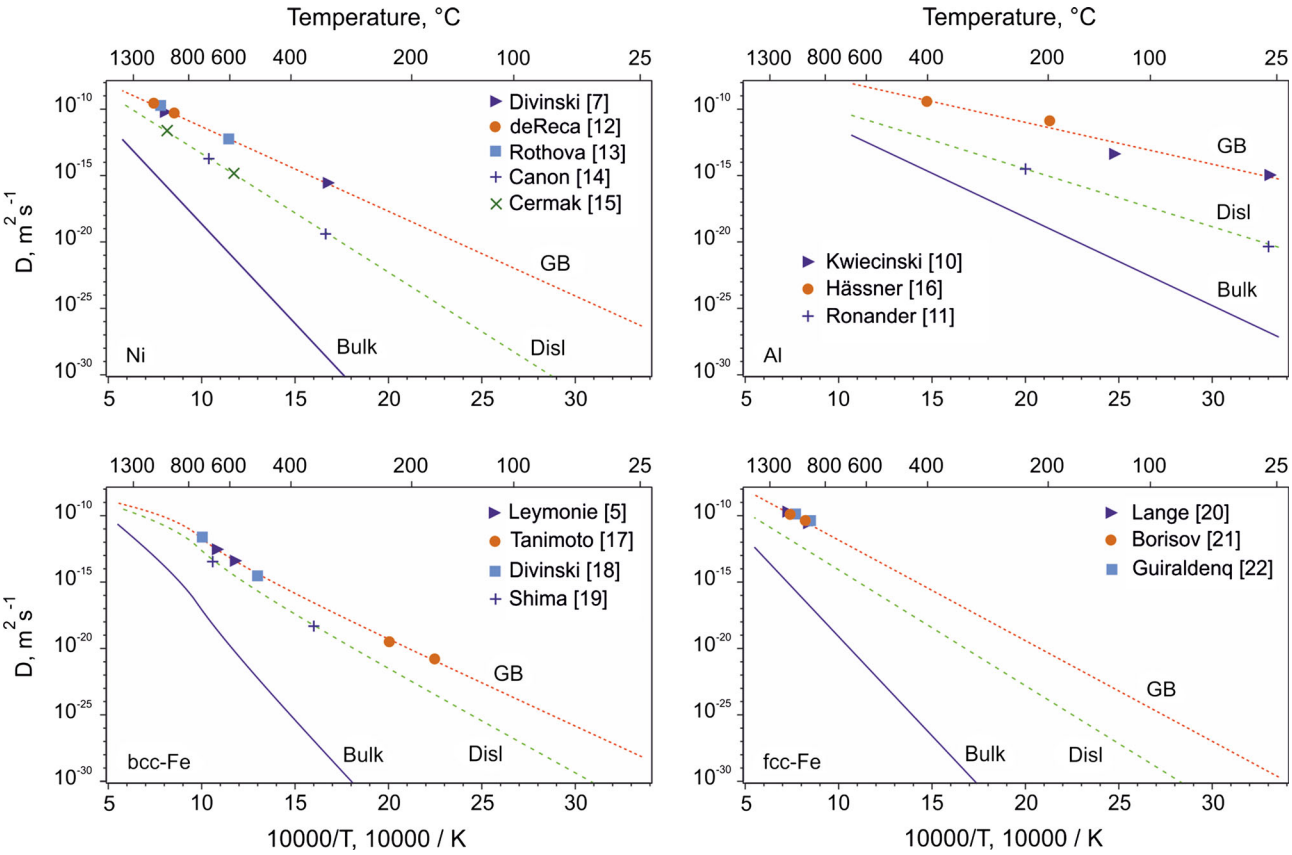

Fig. 1 Arrhenius plots showing the effective self-diffusion rates along grain boundaries (GB), dislocation pipes (Disl), and bulk, respectively, for Ni, Al, and Fe

Table 1 Activation energy and pre-exponential factors as shown in Fig. 1 for Ni, Al, and fcc-Fe

		Q, kJ/mol	D_0, m^2/s	Source
Ni	Bulk	287	2.3×10^{-4}	(Ref 1)
	GB	122	1.2×10^{-5}	This work
	Disl	171	4.0×10^{-5}	This work
Al	Bulk	127.2	1.4×10^{-5}	(Ref 1)
	GB	60.2	2.0×10^{-5}	This work
	Disl	83.2	1.5×10^{-6}	This work
fcc-Fe	Bulk	286	7.0×10^{-5}	(Ref 2)
	GB	145	5.5×10^{-5}	This work
	Disl	167	4.5×10^{-6}	This work

Table 2 Activation energy and pre-exponential factors as shown in Fig. 1 for bcc-Fe

	Low T, RT—693 K		Medium T, 693-1214 K		High T, 1214 K—T_m		
bcc-Fe	Q, kJ/mol	D_0, m^2/s	Q, kJ/mol	D_0, m^2/s	Q, kJ/mol	D_0, m^2/s	Source
Bulk	285	6.0×10^{-4}	330	1.5	240	2×10^{-4}	Fitted from (Ref 3)
GB	125	6.0×10^{-7}	170	1.5×10^{-3}	80	2×10^{-7}	This work
Disl	150	1.5×10^{-6}	195	3.8×10^{-3}	105	5×10^{-7}	This work

Table 3 Chemical composition of alloys (in wt.%)

Lit.	Al	N	C	O
Ref 29	0.046	0.0067	0.001	0.049
Ref 30	0.055	0.024	0.18	···

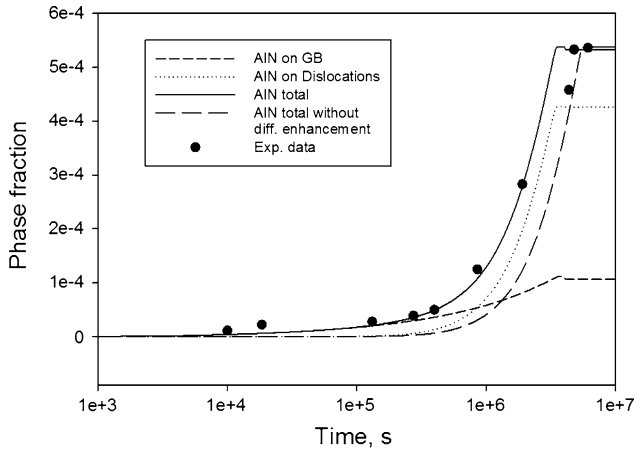

Fig. 2 Phase fraction evolution of AlN in ferrite at 500 °C in a microalloyed steel (Ref 29) with 0.046 wt.% Al and 0.0067 wt.% N, determined by thermoelectric power measurements

precipitation at grain boundaries according to the model that has been developed recently by Kozeschnik et al. (Ref 27), utilizing the grain boundary diffusion coefficient as one of the key input parameters. Dislocation pipe diffusion enters the simulations in determining the number of potential nucleation sites for precipitation as well as accelerating diffusion in terms of the effective diffusion coefficients. The exact treatment of this effect is described in (Ref 28). Since the diffusivity of interstitial N is significantly faster than the diffusivity of the substitutional element Al, we consider Al as the rate-controlling element for diffusion-controlled growth of AlN. Consequently,

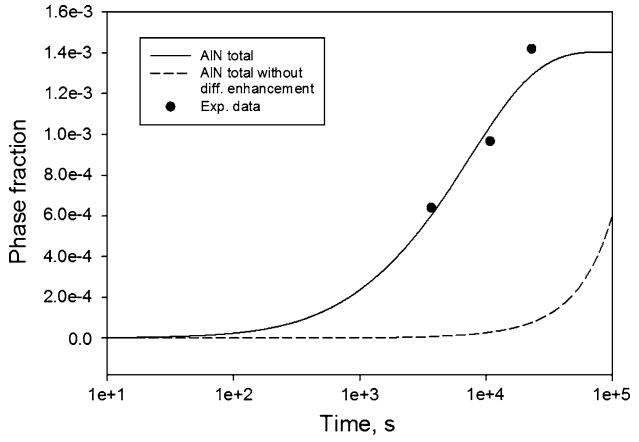

Fig. 3 Phase fraction evolution of AlN in austenite at 1100 °C in a microalloyed steel (Ref 30) with 0.055 wt.% Al and 0.024 wt.% N, determined by analytical chemistry

the effect of heterogeneous diffusion is only taken into account for the substitutional element Al. The chemical composition used in the simulations is given in Table 3.

Figures 2 and 3 show the experimental phase fraction of AlN together with the simulated curves for precipitation on grain boundaries and dislocations, respectively. In determining the experimental phase fractions, Brahmi and Borelly (Ref 29) performed annealing in silica capsules containing low He pressures in salt baths and air furnaces and low-temperature aging in oil baths. König and Scholz (Ref 30) performed annealing in salt baths and air furnaces. In the simulations, precipitates of AlN are considered in two populations nucleating at grain boundaries and dislocations, respectively. Values for grain boundary size and dislocation density of 7.5 μm and 10^{12} (m^{-2}) for ferrite, and 50 μm and 10^{11} (m^{-2}) for austenite, consider the actual sample microstructure and have been used in simulations before (Ref 31). To demonstrate the effect of heterogeneous diffusion on the precipitate evolution, the phase fraction calculated with the proposed values is compared to no diffusion enhancement at grain boundaries and dislocations.

Both figures show clearly the high impact and importance of the assessed diffusion ratios.

5. Summary

Diffusion along grain boundaries and dislocation pipes is significantly faster than bulk diffusion. The ratio comparing diffusion along these short-circuit paths with the bulk values is a main input parameter for thermokinetic simulations, concerning the nucleation and growth of precipitates. Compared to previously used estimates, mainly based on crystallographic structure, the major improvement of our proposed diffusion ratios is the reproduction of available literature data in the form of representative mean values. The evaluation of diffusivity in each system, Al, Fe, and Ni, by a least mean square fit delivers the activation energy Q and pre-exponential factor D_0 between room temperature up to the melting temperature.

It is demonstrated that the simulation of heterogeneous AlN precipitation in microalloyed steel delivers accurate results. In the simulations, two populations of precipitates, nucleating on grain boundaries and dislocation pipes, respectively, are considered. Only if short-circuit diffusion is taken into account, the experimental data can be reproduced in a satisfactory manner.

Acknowledgment

Financial support by the Austrian Federal Government (in particular from the Bundesministerium für Verkehr, Innovation und Technologie and the Bundesministerium für Wirtschaft, Familie und Jugend) and the Styrian Provincial Government, represented by Österreichische Forschungsförderungsgesellschaft mbH and by Steirische Wirtschaftsförderungsgesellschaft mbH, within the research activities of the K2 Competence Centre on "Integrated Research in Materials, Processing and Product Engineering," operated by the Materials Center Leoben Forschung GmbH in the framework of the Austrian COMET Competence Centre Programme, is gratefully acknowledged.

References

1. C.E. Campbell and A.L. Rukhin, Evaluation of Self-Diffusion Data Using Weighted Means Statistics, *Acta Mater.*, 2011, **59**(13), p 5194–5201
2. J. Fridberg, L.-E. Törndahl, and M. Hillert, Diffusion in Iron, *Jernkont. Ann.*, 1969, **153**, p 263–276
3. B. Jönsson, On Ferromagnetic Ordering and Lattice Diffusion—A Simple Model, *Z. Metallkd.*, 1992, **83**(5), p 349–355
4. I. Kaur and W. Gust, 12 Grain and interphase boundary diffusion, In: *Landolt-Börnstein—Group III Condensed Matter: Numerical Data and Functional Relationships in Science and Technology, Volume 26: Diffusion in Solid Metals and Alloys*, Springer Materials, 2012
5. C. Leymonie, Y. Adda, A. Kirianenko, and P. Lacombe, Nouvelle determination des constantes d'autodiffusion intergranulaire du fer cubique centre, *C.R. Acad. Sci. Paris*, 1959, **248**, p 1512–1515
6. H. Hänsel, L. Stratmann, H. Keller, and H.J. Grabke, Effects of the Grain Boundary Segregants Phosphorus, Sulfur, Carbon and Nitrogen on the Grain Boundary Self-Diffusivity in Alpha-Iron, *Acta Metall.*, 1985, **33**(4), p 659–665
7. S.V. Divinski, G. Reglitz, and G. Wilde, Grain Boundary Self-Diffusion in Polycrystalline Nickel of Different Purity Levels, *Acta Mater.*, 2010, **58**(2), p 386–395
8. T. Surholt and C. Herzig, Grain Boundary Self-Diffusion in Cu Polycrystals of Different Purity, *Acta Mater.*, 1997, **45**(9), p 3817–3823
9. N.L. Peterson, Self-Diffusion in Pure Metals, *J. Nucl. Mater.*, 1978, **69&70**, p 3–37
10. J. Kwiecinski and J.W. Wyrzykowski, Investigation of Grain Boundary Self-Diffusion at Low Temperatures in Polycrystalline Aluminium by Means of the Dislocation Spreading Method, *Acta Metall. Mater.*, 1991, **39**(8), p 1953–1958
11. E. Ronander and S. Kritzinger, A Quantitative Study of Anomalous Annealing Phenomena in Quenched Aluminum, *J. Appl. Phys.*, 1978, **49**(7), p 3980–3986
12. N.W. de Reca and C.A. Pampillo, Grain Boundary Diffusivity Via Bulk Diffusion Measurements During Grain Growth, *Scripta Metall. Mater.*, 1975, **9**(12), p 1355–1361
13. V. Rothova, J. Bursik, M. Svoboda, and J. Cermak, Grain Boundary Self-Diffusion in Nickel, *Defect Diffus. Forum*, 2007, **263**, p 207–212
14. R.F. Canon and J.P. Stark, Grain Boundary Self-Diffusion in Nickel, *J. Appl. Phys.*, 1969, **40**(11), p 366–373
15. J. Cermak and Z. Cochnar, Self-Diffusion of ^{63}Ni Along Dislocations, *Mater. Sci. Eng.*, 1994, **174**(1), p 9–13
16. A. Hässner, Untersuchung der Korngrenzdiffusion von Zn-65 in alpha-Aluminium-Zink-Legierungen, *Krist. Tech.*, 1974, **9**(12), p 1371–1388
17. H. Tanimoto, P. Farber, R. Würschum, R.Z. Valiev, and H.-E. Schaefer, Self-Diffusion in High-Density Nanocrystalline Fe, *Nanostruct. Mater.*, 1999, **12**(5), p 681–684
18. S.V. Divinski, J. Geise, E. Rabkin, and C. Herzig, Grain Boundary Self-Diffusion in α-Iron of Different Purity: Effect of Dislocation Enhanced Diffusion, *Z. Metallkd.*, 2004, **95**(10), p 945–952
19. Y. Shima, Y. Ishikawa, H. Nitta, Y. Yamazaki, K. Mimura, M. Isshiki, and Y. Iijima, Self-Diffusion Along Dislocations in Ultra High Purity Iron, *Mater. Trans.*, 2002, **43**(2), p 173–177
20. W. Lange, A. Hässner, and G. Mischer, Messung der Korngrenzen-diffusion von Nickel-63 in Nickel und γ-Eisen, *Phys. Stat. Sol.*, 1964, **5**(1), p 63–71
21. V.T. Borisov, V.M. Golikov, and G.V. Scherbedinskiy, Relation Between Diffusion Coefficients and Grain Boundary Energy, *Fiz. Metal. Metalloved.*, 1964, **17**(6), p 881–885
22. P. Guiraldenq and P. Lacombe, Mesure des coefficients d'autodiffusion intergranulaire du fer en phase γ et comparaison avec l'autodiffusion aux joints de grains du fer α, *Acta Metall.*, 1965, **13**(1), p 51–53
23. G. Stechauner and E. Kozeschnik, Unpublished Research, 2013
24. T. Gladman, D. Dulieu, I. D. McIvor, Structure-Property Relationships in High-Strength Microalloyed Steels, In *Proceedings of an International Symposium on High-Strength, Low-Alloy Steels*, Washington DC, USA, October 1975
25. E. Povoden-Karadeniz, Thermodynamic database mc_fe_v2.008.tdb, 2013
26. E. Povoden-Karadeniz, Mobility database mc_fe_v2.000_prebeta_004, 2013
27. E. Kozeschnik, J. Svoboda, R. Radis, and F.D. Fischer, Mean-Field Model for the Growth and Coarsening of Stoichiometric Precipitates at Grain Boundaries, *Model. Simul. Mater. Sci.*, 2010, **18**(1), p 1–19
28. R. Radis and E. Kozeschnik, Numerical Simulation of NbC Precipitation in Microalloyed Steel, *Model. Simul. Mater. Sci.*, 2012, **20**(5), p 1–15
29. A. Brahmi and R. Borrelly, Study of Aluminium Nitride Precipitation in Pure Fe-Al-N Alloy by Thermoelectric Power Measurements, *Acta Mater.*, 1997, **45**(5), p 1889–1897
30. P. König, W. Scholz, and H. Ulmer, Wechselwirkung von Aluminium, Vanadium und Stickstoff in aluminiumberuhigten, mit Vanadin und Stickstoff legierten schweißbaren Baustählen mit rd. 0.2 % C und 1.5 % Mn, *Archiv für das Eisenhüttenwesen*, 1961, **32**(8), p 541–556
31. R. Radis and E. Kozeschnik, Kinetics of AlN Precipitation in Microalloyed Steel, *Model. Simul. Mater. Sc.*, 2010, **18**(5), p 1–16